



Published in final edited form as:

*Brain Behav Immun.* 2024 January ; 115: 535–542. doi:10.1016/j.bbi.2023.11.007.

## Microglia-mediated calcium-permeable AMPAR accumulation in the nucleus accumbens drives hyperlocomotion during cocaine withdrawal

Ingrid Reverte<sup>1,2,#</sup>, Claudia Marchetti<sup>1,2,#</sup>, Sara Pezza<sup>1,2</sup>, Soami F. Zenoni<sup>1,2</sup>, Giorgia Scaringi<sup>1,2</sup>, Laura Ferrucci<sup>1,2</sup>, Ginevra D'Ottavio<sup>1,2</sup>, Annabella Pignataro<sup>2,3</sup>, Diego Andolina<sup>2,4</sup>, Marcello Raspa<sup>5</sup>, Ferdinando Scavizzi<sup>5</sup>, Marco Venniro<sup>6</sup>, Leslie A. Ramsey<sup>7</sup>, Cornelius Gross<sup>8</sup>, Daniele Caprioli<sup>1,2,\*</sup>, Davide Ragozzino<sup>1,2</sup>

<sup>1</sup>Department of Physiology and Pharmacology, Sapienza University, Laboratory affiliated to Institute Pasteur Italia - Fondazione Cenci Bolognetti, Rome, Italy

<sup>2</sup>IRCCS Santa Lucia Foundation, Rome, Italy

<sup>3</sup>Institute of Translational Pharmacology, National Research Council, CNR, Rome, Italy.

<sup>4</sup>Department of Psychology, Sapienza University of Rome, Rome, Italy

<sup>5</sup>National Research Council, Institute of Biochemistry and Cell Biology (CNR-IBBC/EMMA/Infrafrontier/IMPC), International Campus "A. Buzzati-Traverso", Monterotondo (Rome), Italy

<sup>6</sup>Department of Neurobiology, University of Maryland School of Medicine, Baltimore, USA

<sup>7</sup>Behavioral Neuroscience Research Branch, Intramural Research Program, Baltimore NIDA, NIH, USA

<sup>8</sup>Epigenetics and Neurobiology Unit, European Molecular Biology Laboratory (EMBL), Monterotondo, Italy.

### Abstract

During withdrawal from cocaine, calcium permeable-AMPA receptors (CP-AMPA) progressively accumulate in nucleus accumbens (NAc) synapses, a phenomenon linked to behavioral sensitization and drug-seeking. Recently, it has been suggested that neuroimmune alterations might promote aberrant changes in synaptic plasticity, thus contributing to substance abuse-related behaviors. Here, we investigated the role of microglia in NAc neuroadaptations after withdrawal from cocaine-induced conditioned place preference (CPP). We depleted microglia

\*Corresponding author: Daniele Caprioli (daniele.caprioli@uniroma1.it).

#authors contributed equally to this work

Author contributions

I.R., C.M., D.C.: conception and design; I.R., C.M., A.P., S.P., G.S., L.F., S.F.Z.: data acquisition and analysis; I.R., D.C., D.R., D.A., A.P., M.R., F.S., M.V., L.R., C.G.: data interpretation; and I.R., C.M. and D.C.: writing paper.

**Publisher's Disclaimer:** This is a PDF file of an unedited manuscript that has been accepted for publication. As a service to our customers we are providing this early version of the manuscript. The manuscript will undergo copyediting, typesetting, and review of the resulting proof before it is published in its final form. Please note that during the production process errors may be discovered which could affect the content, and all legal disclaimers that apply to the journal pertain.

Conflict of interest

The authors declare that they have no conflict of interests.

using PLX5622-supplemented diet during cocaine withdrawal, and after the place preference test, we measured dendritic spine density and the presence of CP-AMPA in the NAc shell. Microglia depletion prevented cocaine-induced changes in dendritic spines and CP-AMPA accumulation. Furthermore, microglia depletion prevented conditioned hyperlocomotion without affecting drug-context associative memory. Microglia displayed fewer number of branches, resulting in a reduced arborization area and microglia control domain at late withdrawal. Our results suggest that microglia are necessary for the synaptic adaptations in NAc synapses during cocaine withdrawal and therefore represent a promising therapeutic target for relapse prevention.

## Keywords

microglia; CP-AMPA; nucleus accumbens; dendritic spines; cocaine; drug addiction; drug withdrawal

## Introduction

Chronic cocaine exposure in rodents causes long-lasting changes in excitatory synaptic transmission onto medium-spiny neurons (MSN) of the nucleus accumbens (NAc). Exposure to cocaine initially promotes the emergence of silent synapses lacking functional AMPA receptors (Huang et al., 2009). During withdrawal from cocaine, silent synapses progressively mature by incorporating CP-AMPA receptors, increasing the strength of NAc synapses (Conrad et al., 2008). CP-AMPA receptors accumulation in NAc MSNs has been associated with the appearance of drug-induced behavioral adaptations (i.e. locomotor sensitization and incubated craving), thus contributing to the maintenance of addictive behaviors and heightened propensity of relapse (Wolf, 2016; Wright et al., 2020). To date, studies of cocaine addiction have mostly focused on neuronal mechanisms, despite a body of work that increasingly recognizes the contribution of glial cells, including astrocytes and microglia, to the development and maintenance of drug addiction (Gipson et al., 2021; Lacagnina et al., 2016; McGrath and Briand, 2019). This is an important gap in knowledge because studies on the interplay between glia and synaptic plasticity in the context of cocaine addiction may reveal novel targets for relapse prevention.

Microglia, the main immune cells of the central nervous system, are critical regulators of excitatory synaptic function (Basilico et al., 2022b), and alterations in microglia dysregulate synaptic plasticity mechanisms contributing to neuropsychiatric disorders (Basilico et al., 2022a). Cocaine induces microglia reactivity through signaling at innate immune receptors, which might in turn induce the secretion of soluble factors (e.g. TNF- $\alpha$ ). Indeed, altered serum and brain immune factors have been observed both in people with substance use disorder (SUD) and animal models of SUD (Gipson et al., 2021; Lacagnina et al., 2016). In mice, cocaine-induced release of TNF- $\alpha$  from microglia contributes to the initial depression of glutamatergic synaptic strength in the NAc (Lewitus et al., 2016). However, it is not known whether interactions between microglia and glutamatergic plasticity occur during cocaine withdrawal. In the present study, we sought to investigate whether microglia contribute to the synaptic changes that occur in NAc MSN following a period of withdrawal from cocaine exposure. By depleting microglia using a PLX5622-supplemented diet

following cocaine-induced CPP in mice, we demonstrated that microglia are necessary for the maturation of synapses and CP-AMPA accumulation in the NAc shell driving conditioned hyperlocomotion.

## Methods

### Animals and chemicals

Adult male C57BL/6/J mice (EMMA, Rome, Italy) and Cx3cr1::CreER; RC::LSL-tdTomato mice (EMBL, Monterotondo, Italy) mice were housed 2–4 per cage under a 12-h light/dark cycle (7 am – 7 pm). Experiments were performed during the light cycle. Food and water were provided *ad libitum*. All experiments were carried out in accordance with the Italian Law (DL 26/2014) and European Communities Council Directives (2010/63/UE).

Cocaine-HCl (Sigma-Aldrich) was dissolved in saline (0.9% NaCl) and injected intra-peritoneally (i.p.; 20 mg/kg). Microglia were pharmacologically depleted by the administration of PLX5622 (Plexxikon Inc), a selective inhibitor of CSF1R, essential for microglial proliferation and survival (Elmore et al., 2014; Spangenberg et al., 2019), formulated in standard chow at 1200 ppm (Research Diets Inc). Drug-free standard chow (Research Diets) was provided to control mice. Tamoxifen (Sigma T5648-1G) was dissolved in corn oil at 10 mg/mL and administered intraperitoneally (i.p., 1 mg per 25 g of mouse body-weight) to Cx3cr1::CreER; RC::LSL-tdTomato mice to induce Cre-mediated recombination one week before the start of experimental procedures.

### Conditioned Place Preference (CPP)

The CPP apparatus consisted of two PVC compartments (15×15×20 cm) with different shape and wall pattern design, connected by a central alley. Mice were first habituated to saline i.p. injections for 3 days. On day 1 (pre-test), mice were allowed to explore the entire apparatus (20 min). Mice with a baseline preference of >75% for either compartment were excluded. During conditioning (10 days) mice received cocaine injections (20 mg/kg) paired with the less-preferred compartment during pre-test and saline injections paired with the other compartment, on alternating days (40 min)(Orsini et al., 2005). One day after conditioning we performed a test (WD1) by allowing mice to freely explore the apparatus (20 min), which was repeated after 20 days of cocaine withdrawal (WD21). Behavioral data was analyzed with ANY-Maze 7.16 (Stoelting Co). Place preference score during tests was calculated as time paired-compartment × total time/(total time – time central-area) and normalized by subtracting the baseline preference, so that positive values represent preference and negative values represent aversion (Shukla et al., 2017).

### Analysis of microglia density

Microglia can be identified by the specific cytoplasmic marker ionized calcium-binding adapter molecule 1 (Iba1) detected by immunocytochemical methods (Ito et al., 1998; Paolicelli et al., 2022; Shapiro et al., 2009). After the test mice were anesthetized with Zoletil (80 mg/kg)/ Xylazine (10 mg/kg) mixture and perfused transcardially with 0.1 M phosphate-buffered saline (PBS) followed by 4% paraformaldehyde (PFA). Brains were postfixed with PFA (24 h) and 30% sucrose in PBS (48 h) before being snap frozen. Coronal

sections (40  $\mu\text{m}$ ) were obtained with a Leica cryostat and stored in cryoprotectant solution ( $-20\text{ }^{\circ}\text{C}$ ). Sections were stained with the primary antibody anti-Iba1 (Wako 019–19741; 1:600) and the secondary antibody Goat anti-Rabbit IgG H+L Alexa-Fluor 568 (Abcam ab175471; 1:500) as previously described (Basilico et al., 2022b). Images were acquired with a Fluorescence Olympus BX51 microscope (20x objective). Iba1+ cells were manually identified and annotated with ROI manager of Image J (National Institutes of Health (NIH), USA). We confirmed that selected cells contained a nucleus (DAPI+). Microglial density was reported as number of Iba1+ cells per acquired area ( $\text{microglia}/\text{mm}^2$ ).

### Analysis of microglia morphology

Cx3cr1::CreER; RC::LSL-tdTomato mice (Weinhard et al., 2018) were used to assess microglia morphology. These mice express tdTomato in microglia which enables higher quality imaging relative to immunostaining, where fluorescent background makes more difficult the detection of small processes and morphological reconstruction. In these mice, Cx3cr1::CreER is expressed in heterozygous state, and therefore microglia maintain functional CX3CR1 expression. After the tests, mice were anesthetized and transcardially perfused as reported above. Coronal sections (40  $\mu\text{m}$ ) containing the NAc shell were imaged using a 800LSM Zeiss confocal microscope with a 63x-oil objective (z-interval:0.5  $\mu\text{m}$ ). Cell morphology was reconstructed using Imaris 7.6.5 software (Bitplane Scientific ltd) and then images were transferred to ImageJ (NIH, USA) for analysis. Only cells whose soma and processes were entirely contained in the image were included in the analysis. For each cell, the soma area, the microglia domain and the arborization domains were measured. Through skeleton analysis, we calculated the number and length of microglial processes (Basilico et al., 2022b). For the quantification of microglia density Z-stack images (z-interval: 1  $\mu\text{m}$ ) of NAc shell were acquired using a 20X objective. TdTomato+ cells were manually identified and annotated with Image J ROI manager. Microglial density was reported as number of cells per acquired volume ( $\text{microglia}/\text{mm}^3$ ).

### Analysis of spine density and morphology

Immediately after the behavioral tests, mice were anesthetized with Zoletil (80 mg/kg)/Xylazine (10 mg/kg) mixture and perfused transcardially with 0.1M PBS. Brains were dissected and impregnated using a Golgi–Cox solution as previously described (Glaser and Van der Loos 1981, Izzo, et al. 1987). Brains were sectioned in a 5% sucrose solution to obtain 150  $\mu\text{m}$  thick coronal slices, and stained as previously described (Pignataro et al., 2015). Spine density and morphology were measured in second or third order dendrites from NAc shell and core MSNs (Paxinos, George and Franklin, 2004). Neurons were visualized using a Zeiss Axiophot 2 microscope and selected according to criteria defined by (Restivo et al., 2009). The analysis was performed by an experimenter blind to the experimental conditions. Quantification of spine density was performed using NeuroLucida Explorer software (MBF Bioscience). Z-stack images (z-interval: 0.5  $\mu\text{m}$ ) of dendritic segments (20  $\mu\text{m}$ -length; 4–5 per neuron) were acquired using a 63X/1.4 N.A Plan-Apochromat oil immersion objective and the software MOTIC. Spine head width was measured with Image J software (NIH, USA) considering the maximum diameter of the spine head (at least 1800 measurements were made from each condition).

## Electrophysiology

Immediately after the behavioral tests, mice were decapitated under halothane anesthesia (Sigma-Aldrich). We prepared 250- $\mu\text{m}$  thick coronal brain slices with a vibratome (DSK) in ice-cold cutting solution (135 mM N-methyl-D-glucamine, 1 mM KCl, 1.2 mM  $\text{KH}_2\text{PO}_4$ , 1.5 mM  $\text{MgCl}_2 \cdot 6\text{H}_2\text{O}$ , 0.5 mM  $\text{CaCl}_2 \cdot 2\text{H}_2\text{O}$ , 10 mM D-glucose, and 20 mM choline bicarbonate) continuously oxygenated with (v/v) 95%  $\text{O}_2$  and (v/v) 5%  $\text{CO}_2$ . We then transferred the slices in aCSF solution (119 mM NaCl, 2.5 mM KCl, 1 mM  $\text{NaH}_2\text{PO}_4$ , 26 mM  $\text{NaHCO}_3$ , 1.3 mM  $\text{MgCl}_2$ , 2.5 mM  $\text{CaCl}_2$  and 20 mM D-glucose) saturated with 95% (v/v)  $\text{O}_2$  and 5% (v/v)  $\text{CO}_2$  (Shukla et al., 2017). Before use, slices were allowed to recover for at least 1h at room temperature ( $24 \pm 1^\circ\text{C}$ ).

Standard whole-cell patch-clamp recordings were performed in voltage-clamp mode. Slices were held in a chamber with oxygenated aCSF perfusion at 2 ml/min at room temperature. NAc shell MSNs were identified visually with an upright microscope (Axioskope) equipped with a 40x water-immersion objective (Achromplan Carl Zeiss) and a digital camera (SensiCam). We recorded evoked excitatory postsynaptic currents (EPSCs) from MSN neurons using a patch clamp amplifier (Axopatch 200A, Molecular Devices, LLC). Data were filtered at 2 kHz, digitized (10 kHz), acquired using pClamp 10.0 software and analyzed offline using Clampfit 10 (Molecular Devices). Borosilicate glass pipettes (3–5 M $\Omega$ ) were filled with Cs-based intracellular solution containing: (117.5 mM  $\text{CsMeSO}_3\text{H}$ , 10 mM HEPES, 17.75 mM CsCl, 10 mM TEA-Cl, 0.25 mM EGTA, 10 mM glucose, 2 mM  $\text{MgCl}_2 \cdot 6\text{H}_2\text{O}$ , 4 mM  $\text{Na}_2\text{ATP}$ , 0.3 mM NaGTP, 5 mM QX-314 chloride, 100  $\mu\text{M}$  spermine, pH 7.1, 290 mOsm). Electrical stimulation of NAc slices was done using double-barreled theta glass bipolar electrodes filled with aCSF connected to a stimulus isolation unit (Iso-stim A320, WPI). Synaptic responses were evoked by stimulating for 100  $\mu\text{s}$  at 0.1 Hz; the stimulus intensity was adjusted in order to obtain an amplitude of EPSCs corresponding to approximately the 50% of the maximum response (~50–200 pA). Bicuculline methochloride (HelloBio, HB0895; 10  $\mu\text{M}$ ) and D-APV (HelloBio, HB0225; 50  $\mu\text{M}$ ) were added to the extracellular solution to block  $\text{GABA}_A$  and NMDA receptors respectively. AMPA-mediated EPSC were evoked at  $-70$  mV and  $+40$  mV. The rectification index calculated using the equation:  $\text{RI} = (\text{EPSC amplitude at } -70 \text{ mV} / (-70 - E_{\text{rev}})) / (\text{EPSC amplitude at } +40 \text{ mV} / (40 - E_{\text{rev}}))$  (Kamboj et al., 1995). RI is expressed as a ratio that will increase when rectification increases.

## Statistical analysis

Data were analyzed with SPSS Statistics 25 (IBM). Behavioral data were analyzed as repeated measures ANOVA using the within-subjects factor Withdrawal Day (WD1, WD21) and the between-subjects factors Drug (saline, cocaine) and Diet (control, PLX). Two-way ANOVA with the factors Drug (saline, cocaine) and Diet (control, PLX) was used to analyze microglia density, spine density, rectification index and behavioral data on WD21. Spine head diameter was analyzed by Kolmogorov-Smirnov test for cumulative distributions and one-way ANOVA using the between-subjects factor Group (saline control, cocaine control, saline PLX and cocaine PLX) for the averaged head diameter at WD21. Behavioral data and microglia morphology in transgenic mice were analyzed by two-way ANOVA using the between-subjects factor Withdrawal Day (WD1, WD21) and Drug (saline, cocaine). Where

significant interactions were found, we performed Tukey's HSD post hoc tests. Statistical significance was assumed when  $p < 0.05$ . Data are presented as the mean  $\pm$  SEM.

## Results and Discussion

First, we investigated whether microglia depletion during cocaine withdrawal influences the expression of CPP. Briefly, we trained mice for cocaine CPP (10 days) and tested them after 1 or 21 days of withdrawal (WD). After the test on WD1, we depleted microglia by administering a diet supplemented with the CSF1R-inhibitor PLX5622 and kept the mice on this diet during the withdrawal period (20 days) (Fig. 1A). Notably, we have previously shown that PLX5622 treatment induce an effective microglia depletion of around 80% after 3 days, and around 90% after 7 days, in absence of evident signs of neuroinflammation (Basilico et al., 2022b). We confirmed that PLX5622-diet depleted 90% of microglia in the NAc shell in both saline- and cocaine-treated mice, as shown by the density of Iba1+ cells on WD21 (Fig. 1B–1D). Similar results were observed in the NAc core (not shown; saline control:  $340.85 \pm 22.4$ , cocaine control:  $384.99 \pm 23.16$ , saline PLX:  $42.03 \pm 7.14$ , cocaine PLX:  $32.91 \pm 7.18$ ;  $F_{(1, 45)} = 383.9$ ,  $p < 0.05$ ).

Conditioning with pairings of cocaine and saline produced a higher preference score than saline alone on WD1, indicating that mice acquired CPP. Place preference in cocaine-treated groups was still expressed on WD21, and microglia depletion with PLX during withdrawal did not affect retention of CPP memory (Fig. 1E–F). Notably, the frequency of crossings and distance traveled increased in cocaine control mice between WD1 and 21, while remained stable in the saline groups (Fig. 1G–J). A similar phenomenon has been described in rats after morphine-induced CPP, and deemed as a measure of incubated craving in the CPP procedure (Sun et al., 2017). In contrast, in cocaine-PLX mice locomotor activity remained stable between WD1 and 21 (Fig. 1G–J), suggesting that microglia functions contribute to conditioned hyperlocomotion (Hotsenpiller et al., 2001). In line with our results, a previous study reported that locomotor sensitization was attenuated, while the acquisition and expression of cocaine CPP were preserved, in mice with previously depleted microglia (da Silva et al., 2021).

Cocaine-induced behavioral alterations are the result of modifications in synaptic connectivity and strength in NAc MSNs. Two critical neuroadaptations observed after protracted cocaine withdrawal are changes in spine morphogenesis and increased synaptic CP-AMPA content (Wolf, 2016; Wright et al., 2020). Therefore, we investigated whether microglia depletion during cocaine withdrawal influence spine density and morphology, as well as CP-AMPA accumulation in NAc shell synapses. Following the same experimental design previously described, we depleted microglia following CPP training and immediately after the test on WD21 we performed either Golgi staining or electrophysiological recordings (Fig. 1A).

Dendritic spines are the sites of most excitatory connections in the central nervous system. Early cocaine withdrawal is associated with the formation of *de novo* thin spines, resulting in increased spine density which typically persist after 20 days of withdrawal. Protracted cocaine withdrawal is also associated with increased size of dendritic spine heads, which

correlates with increased surface AMPA receptor content and synaptic strength (Wolf, 2016; Wright et al., 2020). Accordingly, we found increased spine density in cocaine control mice compared to saline mice (Figs 2A–B). This increment was not observed in cocaine PLX mice (microglia depleted), in which spine density was comparable to saline-control and saline-PLX mice (Figs 2A–B). We also observed higher cumulative frequency of spine heads with large diameters in cocaine control mice, suggesting that withdrawal from cocaine CPP was associated with an increased number of mature spines (Figs 2C–D). In contrast, cocaine PLX mice displayed more spines with smaller head diameter compared to all the other groups (Figs 2C–D), suggesting that new dendritic spines formed after cocaine exposure remained immature in microglia depleted mice. We found similar results in the NAc core (not shown; spine density: saline control:  $1.348 \pm 0.071$ , cocaine control:  $1.755 \pm 0.067$ , saline PLX:  $1.430 \pm 0.057$ , cocaine PLX:  $1.524 \pm 0.055$ , interaction drug x diet:  $F_{(1, 117)} = 6.246$ ,  $p < 0.05$ ; spine diameter: saline control:  $0.5944 \pm 0.0038$ , cocaine control:  $0.6130 \pm 0.0043$ , saline PLX:  $0.6102 \pm 0.0041$ , cocaine PLX:  $0.5548 \pm 0.0041$ , group effect:  $F_{(3, 7988)} = 43.26$ ,  $p < 0.05$ ). Notably, we did not observe differences in spine density and diameter in NAc shell MSNs between saline-control and saline-PLX mice. Our results suggest that during cocaine withdrawal microglia contribute to the maintenance and growth of new immature spines induced by cocaine experience.

We then examined whether microglia contribute to the functional maturation of glutamatergic synapses – via the insertion of CP-AMPA receptors – in NAc synapses during cocaine withdrawal. Microglia modulates excitatory neurotransmission partially by regulating AMPA receptors insertion at synapses, possibly through the release of soluble factors (Lewitus et al., 2016; Parkhurst et al., 2013). We hypothesized that during cocaine withdrawal microglia contribute to CP-AMPA accumulation in NAc synapses. To test this, we recorded evoked AMPAR-mediated excitatory post-synaptic currents in MSNs of NAc shell immediately after the test on WD21 (Fig. 1A). Synaptic insertion of CP-AMPA receptors can be detected by increased rectification of EPSCs at positive membrane potentials, evidenced by an increased rectification index (Shukla et al., 2017; Terrier et al., 2016). According to the literature, we found increased rectification of AMPA EPSCs in cocaine control relative to saline control mice at WD21 after cocaine CPP (Shukla et al., 2017). Mice with depleted microglia (both saline PLX and cocaine PLX) showed linear current–voltage relationships and a rectification index comparable to saline controls. Indeed, the rectification index of cocaine control mice differed significantly from all the other groups including cocaine PLX mice (Fig. 2E–H). As a control we also recorded NAc shell synapses on WD1 and found no differences in the rectification index between saline and cocaine-treated mice; rectification index values on WD1 were comparable to those of saline control mice on WD21 (not shown; saline  $1.37 \pm 0.10$ , cocaine  $1.40 \pm 0.09$ ;  $t_{20} = 0.2229$ ,  $p > 0.05$ ).

These results suggest that microglia contribute to the accumulation of CP-AMPA receptors in the NAc shell during cocaine withdrawal. It remains to be determined whether synapses in cocaine PLX mice (microglia depleted) remain silent or they mature by incorporating CP-AMPA receptors. Our results suggest that synapses remain silent, since dendritic spines in cocaine PLX mice show the smallest diameter sizes (Fig. 2H), and spine size correlates with AMPA receptors content (Wolf, 2016; Wright et al., 2020).

Microglia are dynamic cells that change their morphological and functional properties depending on the surrounding microenvironment (Davalos et al., 2005; De Biase et al., 2017; Hanisch and Kettenmann, 2007). In the healthy brain microglia are highly ramified, with branches surveilling the parenchyma contacting neurons and synapses (Nimmerjahn et al., 2005; Wake et al., 2009). Upon damage or infection microglia adopts a pro-inflammatory and phagocytic phenotype associated to branch retraction and amoeboid morphologies (Hanisch and Kettenmann, 2007).

This raises the question of whether the observed microglia-induced aberrant plasticity during cocaine withdrawal (Fig. 2) is associated with a reactive phenotype in these cells. Reactive microglia has been observed postmortem in humans and primates with a prolonged history of cocaine use (Little et al., 2009; Smith et al., 2019), but not in living cocaine users (Narendran et al., 2014). In rodents, chronic but not acute exposure to cocaine induces changes in microglia morphology, typically a reduction of branches (Burkovetskaya et al., 2020; Cotto et al., 2018; Lewitus et al., 2016; Rodríguez-Arias et al., 2018). We analyzed microglia morphology in mice expressing a fluorescent reporter under the control of the microglial receptor CX3CR1 (Cx3cr1::CreER; RC::LSL-tdTomato mice) (Weinhard et al., 2018). We trained these mice for cocaine CPP (and saline as control) as previously described and tested them either at WD1 or WD21. Transgenic mice showed similar cocaine-induced place preference (both at WD1 and WD21) and higher locomotor activity at WD21 as observed in C57BL6/J mice (Fig. 3A–C). We did not observe changes in microglia morphology on WD1 (Fig. 3). After prolonged cocaine withdrawal (WD21) microglia displayed a reduction in the number of branches, resulting in a reduced arborization area and microglia control domain (Fig. 3G–K). The morphological index (soma area/arborization area) was increased in cocaine exposed mice at WD21 (Fig. 3L). Our results are in contrast with two works reporting no changes in microglia morphology after 10 and 14 days of withdrawal respectively (Lewitus et al., 2016; Wang et al., 2017). Microglia changes following cocaine might depend on the drug administration regimen (Calipari et al., 2018; Cotto et al., 2018; Lewitus et al., 2016) and procedures of extinction and reinstatement (Brown et al., 2018), especially in the NAc. It is therefore possible that in our procedure, exposure to the drug-associated context increases microglia reactivity after prolonged withdrawal. In this regard plasma cytokines are altered in cocaine users after exposure to drug associated cues (Fox et al., 2012).

Together the above results suggest that microglia are necessary for dendritic spine remodeling and CP-AMPA accumulation in NAc synapses during cocaine withdrawal contributing to hyperlocomotion but are not necessary for drug-context memory retrieval. It has been previously reported that NAc accumulation of CP-AMPA is not required for the retrieval of CPP (Panopoulou and Schlüter, 2022; Shukla et al., 2017), but instead modulate the threshold for drug memory retrieval (Panopoulou and Schlüter, 2022) and promote cue-induced cocaine seeking (Conrad et al., 2008). On the other hand, our results suggest that microglia modulation of synaptic plasticity in the NAc shell contributes to the sensitizing effects of drug-associated cues. These results highlight the relevance of microglia function to the development of drug-induced behavioral adaptations and their potential relevance to other critical features of SUD such as incentive motivation, cue-induced cocaine seeking and relapse. Moreover, it has been previously reported that manipulations of

microglia – such as the administration of minocycline, an antibiotic with inhibitory effect on microglial activation, or antagonism of the TLR4 receptor, a receptor primarily expressed by microglia in the brain – attenuate context- and drug- induced psychostimulant reinstatement (Attarzadeh-Yazdi et al., 2014; Brown et al., 2018).

The present study did not address the exact mechanisms of how microglia modulate NAc plasticity during withdrawal. However, we speculate that a plausible mechanism is through the microglial release of soluble factors, such as TNF $\alpha$ , previously reported to regulate CP-AMPA expression in neurons (Beattie et al., 2002; Heir and Stellwagen, 2020; Kleidonas et al., 2022; Lewitus et al., 2016, 2014). Another plausible mediator is microglial-BDNF previously reported to regulate both structural and functional plasticity in cortical excitatory synapses (Parkhurst et al., 2013). Notably, BDNF is also involved in the long-term neuroplasticity associated with incubation of cocaine craving (Li and Wolf, 2015).

An open question for future studies is whether microglia also contribute to CP-AMPA accumulation in female mice. Sex differences have been reported in microglia gene expression and function (Bordeleau et al., 2019; Villa et al., 2018) and neuroimmune modulation in the NAc core, which modulates cue-induced drug-seeking in a sex-specific manner (Namba et al., 2022; Reverte et al., 2022).

In conclusion, we revealed that microglia are necessary to the critical neuroadaptations that occur in NAc shell synapses during cocaine withdrawal. Particularly we uncovered that microglia mediate the maturation of dendritic spines and CP-AMPA accumulation, promoting conditioned hyperlocomotion. These results encourage future studies assessing the relevance of microglia mechanisms to incubated cocaine craving and call attention to the importance of studying microglia as a potential therapeutic target for SUD.

## Acknowledgements

The work was supported by a grant from Istituto Pasteur-Fondazione, Italy (Cenci Bolognetti) to Davide Ragozzino, Italian Ministry of Health (Ricerca Finalizzata, RF-2021-12374450) to Daniele Caprioli and Fondi Ricerca Ateneo from Sapienza University of Rome (2019, RM11916B0E316F23 to Daniele Caprioli; 2020, RG120172B8E2B021 to Davide Ragozzino and Avvio alla Ricerca 2021, AR22117A7CA27DD1 to Ingrid Reverte). Claudia Marchetti, Giorgia Scaringi and Ginevra D'Ottavio were supported by the PhD programs from Sapienza University, Rome. The authors thank Giulia Coccia, Jacopo Modoni, Azka Khan, Sara Ficara and Margherita Ferri for their help during data collection, Alessandro Felici and Arsenio Armagno for help with animal husbandry and Aldo Badiani, Cristina Limatola and Sapienza Technopole for their support. PLX5622 was provided under Materials Transfer Agreement by Plexxikon Inc. (Berkeley, CA).

## References

- Attarzadeh-Yazdi G, Arezoomandan R, Haghparast A, 2014. Minocycline, an antibiotic with inhibitory effect on microglial activation, attenuates the maintenance and reinstatement of methamphetamine-seeking behavior in rat. *Prog. Neuropsychopharmacol. Biol. Psychiatry* 53, 142–148. 10.1016/J.PNPBP.2014.04.008 [PubMed: 24768984]
- Basilico B, Ferrucci L, Khan A, Di Angelantonio S, Ragozzino D, Reverte I, 2022a. What microglia depletion approaches tell us about the role of microglia on synaptic function and behavior. *Front. Cell. Neurosci* 0, 560. 10.3389/FNCEL.2022.1022431
- Basilico B, Ferrucci L, Ratano P, Golia MT, Grimaldi A, Rosito M, Ferretti V, Reverte I, Sanchini C, Marrone MC, Giubettini M, De Turrís V, Salerno D, Garofalo S, St-Pierre MK, Carrier M, Renzi M, Pagani F, Modi B, Raspa M, Scavizzi F, Gross CT, Marinelli S, Tremblay MÈ, Caprioli D, Maggi L,

- Limatola C, Di Angelantonio S, Ragozzino D, 2022b. Microglia control glutamatergic synapses in the adult mouse hippocampus. *Glia* 70, 1–23. 10.1002/glia.24101
- Beattie EC, Stellwagen D, Morishita W, Bresnahan JC, Byeong KH, Von Zastrow M, Beattie MS, Malenka RC, 2002. Control of synaptic strength by glial TNF $\alpha$ . *Science* (80-. ). 295, 2282–2285. 10.1126/SCIENCE.1067859 [PubMed: 11910117]
- Bordeleau M, Carrier M, Luheshi GN, Tremblay MÈ, 2019. Microglia along sex lines: From brain colonization, maturation and function, to implication in neurodevelopmental disorders. *Semin. Cell Dev. Biol* 94, 152–163. 10.1016/J.SEMCDB.2019.06.001 [PubMed: 31201858]
- Brown KT, Levis SC, O'Neill CE, Northcutt AL, Fabisiak TJ, Watkins LR, Bachtell RK, 2018. Innate immune signaling in the ventral tegmental area contributes to drug-primed reinstatement of cocaine seeking. *Brain. Behav. Immun* 67, 130. 10.1016/J.BBI.2017.08.012 [PubMed: 28813640]
- Burkovetskaya ME, Small R, Guo L, Buch S, Guo ML, 2020. Cocaine self-administration differentially activates microglia in the mouse brain. *Neurosci. Lett* 728, 134951. 10.1016/J.NEULET.2020.134951 [PubMed: 32278944]
- Calipari ES, Godino A, Peck EG, Salery M, Mervosh NL, Landry JA, Russo SJ, Hurd YL, Nestler EJ, Kiraly DD, 2018. Granulocyte-colony stimulating factor controls neural and behavioral plasticity in response to cocaine. *Nat. Commun* 9. 10.1038/S41467-017-01881-X [PubMed: 29339724]
- Conrad KL, Tseng KY, Uejima JL, Reimers JM, Heng LJ, Shaham Y, Marinelli M, Wolf ME, 2008. Formation of accumbens GluR2-lacking AMPA receptors mediates incubation of cocaine craving. *Nature* 454, 118–121. 10.1038/NATURE06995 [PubMed: 18500330]
- Cotto B, Li H, Tuma RF, Ward SJ, Langford D, 2018. Cocaine-mediated activation of microglia and microglial MeCP2 and BDNF production. *Neurobiol. Dis* 117, 28–41. 10.1016/j.nbd.2018.05.017 [PubMed: 29859319]
- da Silva MCM, Gomes GF, de Barros Fernandes H, da Silva AM, Teixeira AL, Moreira FA, de Miranda AS, de Oliveira ACP, 2021. Inhibition of CSF1R, a receptor involved in microglia viability, alters behavioral and molecular changes induced by cocaine. *Sci. Rep* 11, 1–15. 10.1038/s41598-021-95059-7 [PubMed: 33414495]
- Davalos D, Grutzendler J, Yang G, Kim JV, Zuo Y, Jung S, Littman DR, Dustin ML, Gan WB, 2005. ATP mediates rapid microglial response to local brain injury in vivo. *Nat. Neurosci* 2005 86 8, 752–758. 10.1038/nn1472
- De Biase LM, Schuebel KE, Fusfeld ZH, Jair K, Hawes IA, Cimbri R, Zhang HY, Liu QR, Shen H, Xi ZX, Goldman D, Bonci A, 2017. Local Cues Establish and Maintain Region-Specific Phenotypes of Basal Ganglia Microglia. *Neuron* 95, 341–356.e6. 10.1016/j.neuron.2017.06.020 [PubMed: 28689984]
- Elmore MRP, Najafi AR, Koike MA, Dagher NN, Spangenberg EE, Rice RA, Kitazawa M, Matusow B, Nguyen H, West BL, Green KN, 2014. Colony-stimulating factor 1 receptor signaling is necessary for microglia viability, unmasking a microglia progenitor cell in the adult brain. *Neuron* 82, 380–397. 10.1016/j.neuron.2014.02.040 [PubMed: 24742461]
- Fox HC, D'Sa C, Kimmerling A, Siedlarz KM, Tuit KL, Stowe R, Sinha R, 2012. Immune system inflammation in cocaine dependent individuals: implications for medications development. *Hum. Psychopharmacol* 27, 156–166. 10.1002/HUP.1251 [PubMed: 22389080]
- Gipson CD, Rawls S, Scofield MD, Siemsen BM, Bondy EO, Maher EE, 2021. Interactions of neuroimmune signaling and glutamate plasticity in addiction. *J. Neuroinflammation* 18, 1–23. 10.1186/s12974-021-02072-8 [PubMed: 33402173]
- Hanisch UK, Kettenmann H, 2007. Microglia: active sensor and versatile effector cells in the normal and pathologic brain. *Nat. Neurosci* 2007 1011 10, 1387–1394. 10.1038/nn1997
- Heir R, Stellwagen D, 2020. TNF-Mediated Homeostatic Synaptic Plasticity: From in vitro to in vivo Models. *Front. Cell. Neurosci* 14. 10.3389/FNCEL.2020.565841 [PubMed: 32116560]
- Hotsenpiller G, Giorgetti M, Wolf ME, 2001. Alterations in behaviour and glutamate transmission following presentation of stimuli previously associated with cocaine exposure. *Eur. J. Neurosci* 14, 1843–1855. 10.1046/J.0953-816X.2001.01804.X [PubMed: 11860480]
- Huang YH, Lin Y, Mu P, Lee BR, Brown TE, Wayman G, Marie H, Liu W, Yan Z, Sorg BA, Schlüter OM, Zukin RS, Dong Y, 2009. In vivo Cocaine Experience Generates Silent Synapses. *Neuron* 63, 40. 10.1016/J.NEURON.2009.06.007 [PubMed: 19607791]

- Ito D, Imai Y, Ohsawa K, Nakajima K, Fukuuchi Y, Kohsaka S, 1998. Microglia-specific localisation of a novel calcium binding protein, Iba1. *Mol. Brain Res* 57, 1–9. 10.1016/S0169-328X(98)00040-0 [PubMed: 9630473]
- Kamboj SK, Swanson GT, Cull-Candy SG, 1995. Intracellular spermine confers rectification on rat calcium-permeable AMPA and kainate receptors. *J. Physiol* 486 ( Pt 2), 297–303. 10.1113/JPHYSIOL.1995.SP020812 [PubMed: 7473197]
- Kleidonas D, Kirsch M, Andrieux G, Pfeifer D, Boerries M, Vlachos A, 2022. Tumor necrosis factor  $\alpha$  modulates excitatory and inhibitory neurotransmission in a concentration-dependent manner. *bioRxiv* 2022.04.14.487444. 10.1101/2022.04.14.487444
- Lacagnina MJ, Rivera PD, Bilbo SD, 2016. Glial and Neuroimmune Mechanisms as Critical Modulators of Drug Use and Abuse. *Neuropsychopharmacol* 2017 421 42, 156–177. 10.1038/npp.2016.121
- Lewitus GM, Konefal SC, Greenhalgh AD, Pribrag H, Augereau K, Stellwagen D, 2016. Microglial TNF- $\alpha$  Suppresses Cocaine-Induced Plasticity and Behavioral Sensitization. *Neuron* 90, 483–491. 10.1016/j.neuron.2016.03.030 [PubMed: 27112496]
- Lewitus GM, Pribrag H, Duseja R, St-Hilaire M, Stellwagen D, 2014. An adaptive role of TNF $\alpha$  in the regulation of striatal synapses. *J. Neurosci* 34, 6146–6155. 10.1523/JNEUROSCI.3481-13.2014 [PubMed: 24790185]
- Li X, Wolf ME, 2015. Multiple faces of BDNF in cocaine addiction. *Behav. Brain Res* 279, 240–254. 10.1016/J.BBR.2014.11.018 [PubMed: 25449839]
- Little KY, Ramssen E, Welchko R, Volberg V, Roland CJ, Cassin B, 2009. Decreased brain dopamine cell numbers in human cocaine users. *Psychiatry Res* 168, 173–180. 10.1016/J.PSYCHRES.2008.10.034 [PubMed: 19233481]
- McGrath AG, Briand LA, 2019. A potential role for microglia in stress- and drug-induced plasticity in the nucleus accumbens: A mechanism for stress-induced vulnerability to substance use disorder. *Neurosci. Biobehav. Rev* 107, 360–369. 10.1016/j.neubiorev.2019.09.007 [PubMed: 31550452]
- Namba MD, Phillips MN, Neisewander JL, Foster Olive M, 2022. Nuclear factor kappa B signaling within the rat nucleus accumbens core sex-dependently regulates cue-induced cocaine seeking and matrix metalloproteinase-9 expression. *Brain. Behav. Immun* 102, 252–265. 10.1016/J.BBI.2022.03.002 [PubMed: 35259426]
- Narendran R, Lopresti BJ, Mason NS, Deutch L, Paris J, Himes ML, Kodavali CV, Nimgaonkar VL, 2014. Cocaine Abuse in Humans Is Not Associated with Increased Microglial Activation: An 18-kDa Translocator Protein Positron Emission Tomography Imaging Study with [<sup>11</sup>C]PBR28. *J. Neurosci* 34, 9945. 10.1523/JNEUROSCI.0928-14.2014 [PubMed: 25057196]
- Nimmerjahn A, Kirchhoff F, Helmchen F, 2005. Resting microglial cells are highly dynamic surveillants of brain parenchyma in vivo. *Neuroforum* 11, 95–96. 10.1515/nf-2005-0304
- Orsini C, Bonito-Oliva A, Conversi D, Cabib S, 2005. Susceptibility to conditioned place preference induced by addictive drugs in mice of the C57BL/6 and DBA/2 inbred strains. *Psychopharmacology (Berl)* 181, 327–336. 10.1007/S00213-005-2259-6/FIGURES/8 [PubMed: 15864555]
- Panopoulou M, Schlüter OM, 2022. Ca<sup>2+</sup>-permeable AMPA receptors set the threshold for retrieval of drug memories. *Mol. Psychiatry* 27, 2868–2878. 10.1038/S41380-022-01505-X [PubMed: 35296806]
- Paolicelli RC, Sierra A, Stevens B, Tremblay ME, Aguzzi A, Ajami B, Amit I, Audinat E, Bechmann I, Bennett M, Bennett F, Bessis A, Biber K, Bilbo S, Blurton-Jones M, Boddeke E, Brites D, Brône B, Brown GC, Butovsky O, Carson MJ, Castellano B, Colonna M, Cowley SA, Cunningham C, Davalos D, De Jager PL, de Strooper B, Denes A, Eggen BJL, Eyo U, Galea E, Garel S, Ginhoux F, Glass CK, Gokce O, Gomez-Nicola D, González B, Gordon S, Graeber MB, Greenhalgh AD, Gressens P, Greter M, Gutmann DH, Haass C, Heneka MT, Heppner FL, Hong S, Hume DA, Jung S, Kettenmann H, Kipnis J, Koyama R, Lemke G, Lynch M, Majewska A, Malcangio M, Malm T, Mancuso R, Masuda T, Matteoli M, McColl BW, Miron VE, Molofsky AV, Monje M, Mracsko E, Nadjar A, Neher JJ, Neniskyte U, Neumann H, Noda M, Peng B, Peri F, Perry VH, Popovich PG, Pridans C, Priller J, Prinz M, Ragozzino D, Ransohoff RM, Salter MW, Schaefer A, Schafer DP, Schwartz M, Simons M, Smith CJ, Streit WJ, Tay TL, Tsai LH, Verkhratsky A, von Bernhardi R, Wake H, Wittamer V, Wolf SA, Wu LJ, Wyss-Coray T, 2022. Microglia states and nomenclature:

- A field at its crossroads. *Neuron* 110, 3458–3483. 10.1016/J.NEURON.2022.10.020 [PubMed: 36327895]
- Parkhurst CN, Yang G, Ninan I, Savas JN, Yates JR, Lafaille JJ, Hempstead BL, Littman DR, Gan WB, 2013. Microglia promote learning-dependent synapse formation through brain-derived neurotrophic factor. *Cell* 155, 1596–1609. 10.1016/J.CELL.2013.11.030 [PubMed: 24360280]
- Paxinos George and Franklin KBJ, 2004. *The mouse brain in stereotaxic coordinates: compact, second ed.* Elsevier Academic Press, Amsterdam, Boston.
- Pignataro A, Borreca A, Ammassari-Teule M, Middei S, 2015. CREB Regulates Experience-Dependent Spine Formation and Enlargement in Mouse Barrel Cortex. *Neural Plast* 2015. 10.1155/2015/651469
- Restivo L, Vetere G, Bontempi B, Ammassari-Teule M, 2009. The formation of recent and remote memory is associated with time-dependent formation of dendritic spines in the hippocampus and anterior cingulate cortex. *J. Neurosci* 29, 8206–8214. 10.1523/JNEUROSCI.0966-09.2009 [PubMed: 19553460]
- Reverte I, D’Ottavio G, Stanislaw Milella M, Caprioli D, 2022. Sex differences in the immune system: Implications for cocaine relapse. *Brain. Behav. Immun* 104, 29–30. 10.1016/J.BBI.2022.05.009 [PubMed: 35580793]
- Rodríguez-Arias M, Montagud-Romero S, Carrión AMG, Ferrer-Pérez C, Pérez-Villalba A, Marco E, Gallardo ML, Viveros MP, Miarro J, 2018. Social stress during adolescence activates long-term microglia inflammation insult in reward processing nuclei. *PLoS One* 13. 10.1371/JOURNAL.PONE.0206421
- Shapiro LA, Perez ZD, Foresti ML, Arisi GM, Ribak CE, 2009. Morphological and ultrastructural features of Iba1-immunolabeled microglial cells in the hippocampal dentate gyrus. *Brain Res* 1266, 29. 10.1016/J.BRAINRES.2009.02.031 [PubMed: 19249294]
- Shukla A, Beroun A, Panopoulou M, Neumann PA, Grant SG, Olive MF, Dong Y, Schlüter OM, 2017. Calcium-permeable AMPA receptors and silent synapses in cocaine-conditioned place preference. *EMBO J* 36, 458–474. 10.15252/embj.201695465 [PubMed: 28077487]
- Smith HR, Beveridge TJR, Nader SH, Nader MA, Porrino LJ, 2019. Regional Elevations in Microglial Activation and Cerebral Glucose Utilization in Frontal White Matter Tracts of Rhesus Monkeys Following Prolonged Cocaine Self-Administration. *Brain Struct. Funct* 224, 1417. 10.1007/S00429-019-01846-4 [PubMed: 30747315]
- Spangenberg E, Severson PL, Hohsfield LA, Crapser J, Zhang J, Burton EA, Zhang Y, Spevak W, Lin J, Phan NY, Habets G, Rymar A, Tsang G, Walters J, Nespi M, Singh P, Broome S, Ibrahim P, Zhang C, Bollag G, West BL, Green KN, 2019. Sustained microglial depletion with CSF1R inhibitor impairs parenchymal plaque development in an Alzheimer’s disease model. *Nat. Commun* 10, 1–21. 10.1038/s41467-019-11674-z [PubMed: 30602773]
- Sun Y, Pan Z, Ma Y, 2017. Increased entrances to side compartments indicate incubation of craving in morphine-induced rat and tree shrew CPP models. *Pharmacol. Biochem. Behav* 159, 62–68. 10.1016/j.pbb.2017.07.007 [PubMed: 28720521]
- Terrier J, Lüscher C, Pascoli V, 2016. Cell-Type Specific Insertion of GluA2-Lacking AMPARs with Cocaine Exposure Leading to Sensitization, Cue-Induced Seeking, and Incubation of Craving. *Neuropsychopharmacology* 41, 1779–1789. 10.1038/NPP.2015.345 [PubMed: 26585289]
- Villa A, Gelosa P, Castiglioni L, Cimino M, Rizzi N, Pepe G, Lolli F, Marcello E, Sironi L, Vegeto E, Maggi A, 2018. Sex-Specific Features of Microglia from Adult Mice. *Cell Rep* 23, 3501–3511. 10.1016/j.celrep.2018.05.048 [PubMed: 29924994]
- Wake H, Moorhouse AJ, Jinno S, Kohsaka S, Nabekura J, 2009. Resting microglia directly monitor the functional state of synapses in vivo and determine the fate of ischemic terminals. *J. Neurosci* 29, 3974–3980. 10.1523/JNEUROSCI.4363-08.2009 [PubMed: 19339593]
- Wang ZJ, Martin JA, Gancarz AM, Adank DN, Sim FJ, Dietz DM, 2017. Activin A is increased in the nucleus accumbens following a cocaine binge. *Sci. Reports* 2017 7, 1–8. 10.1038/srep43658
- Weinhard L, Di Bartolomei G, Bolasco G, Machado P, Schieber NL, Neniskyte U, Exiga M, Vadisiute A, Raggioli A, Schertel A, Schwab Y, Gross CT, 2018. Microglia remodel synapses by presynaptic trogocytosis and spine head filopodia induction. *Nat. Commun* 9, 1228. 10.1038/s41467-018-03566-5 [PubMed: 29581545]

- Wolf ME, 2016. Synaptic mechanisms underlying persistent cocaine craving. *Nat. Rev. Neurosci* 2016 17(6), 351–365. [10.1038/nrn.2016.39](https://doi.org/10.1038/nrn.2016.39)
- Wright WJ, Graziane NM, Neumann PA, Hamilton PJ, Cates HM, Fuerst L, Spenceley A, MacKinnon-Booth N, Iyer K, Huang YH, Shaham Y, Schlüter OM, Nestler EJ, Dong Y, 2020. Silent synapses dictate cocaine memory destabilization and reconsolidation. *Nat. Neurosci* 23, 32–46. [10.1038/s41593-019-0537-6](https://doi.org/10.1038/s41593-019-0537-6) [PubMed: 31792465]

Author Manuscript

Author Manuscript

Author Manuscript

Author Manuscript

**Highlights**

- Microglia depletion prevented cocaine-induced increases in NAc dendritic spines and CP-AMPA
- Microglia depletion prevented cocaine-induced conditioned hyperlocomotion
- Microglia displayed reduced arborization area and control domain at late withdrawal
- Microglia are necessary for the synaptic adaptations in NAc synapses during cocaine withdrawal

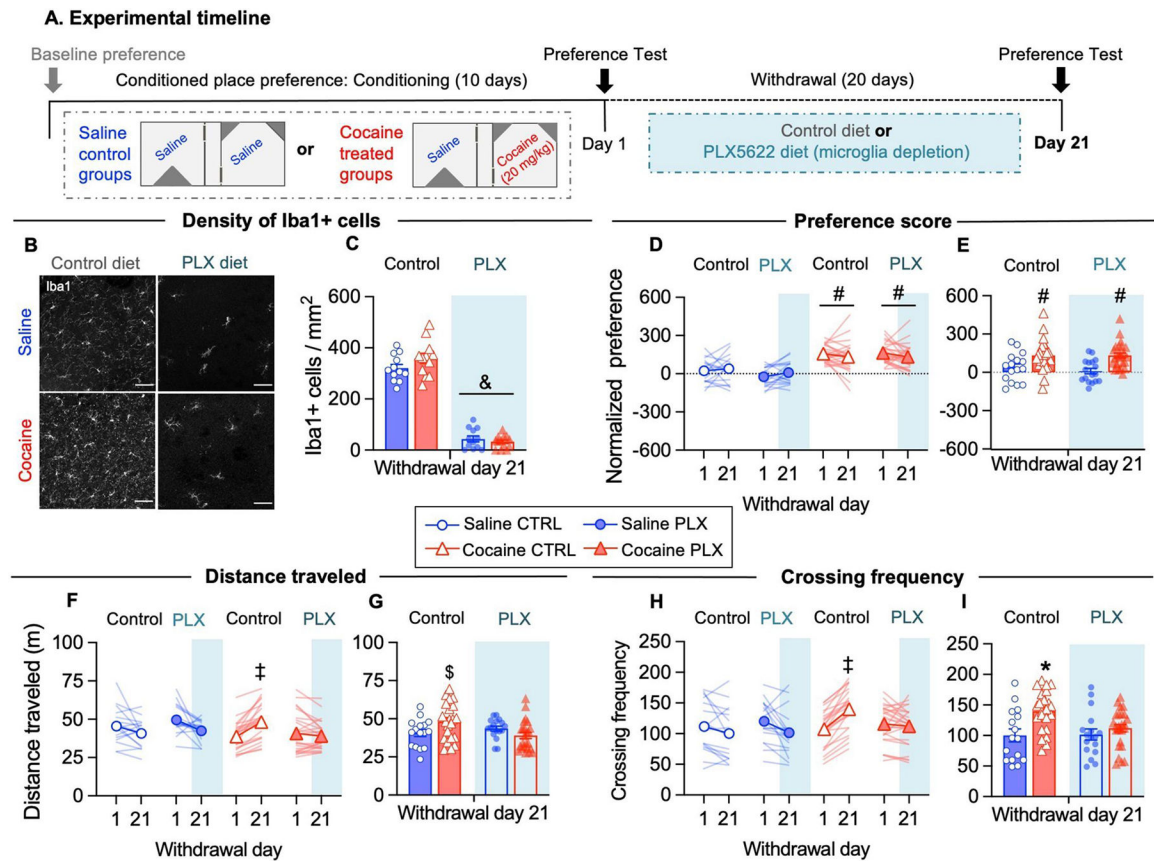


**Figure 1. Microglia depletion during cocaine withdrawal prevents conditioned hyperlocomotion without affecting conditioned place preference memory.**

(A) Schematic of the protocol schedule for cocaine induced CPP training, testing and microglia depletion during withdrawal. (B) Representative images of Iba1+ immunofluorescence labeling in the NAC shell at WD21 under the indicated conditions. Nuclei were counterstained with DAPI (not shown). (C) The density of Iba1+ cells was significantly reduced in both saline- and cocaine- treated mice after 20 days of PLX5622 supplemented diet (Diet:  $F_{(1, 45)} = 465.0$ ,  $p < 0.05$ ;  $N = 12$  fields/4 mice per group). (D) Place preference score was higher in cocaine-treated mice than saline-treated mice both at WD1 and at WD21 (Drug:  $F_{(1, 77)} = 56.95$ ,  $p < 0.05$ ) independently of PLX5622 treatment. (E) Place preference score at WD21 time point (Drug:  $F_{(1, 77)} = 20.07$ ,  $p < 0.05$ ). (F) The distance traveled in the apparatus during tests increases from WD1 to WD21 in cocaine control mice (interaction Drug x Diet x WD:  $F_{(1, 77)} = 4.960$ ,  $p < 0.05$ ). (G) Distance traveled during test at WD21 time point (interaction Drug x Diet:  $F_{(1, 77)} = 5.456$ ,  $p < 0.05$ ). (H) The frequency of crossings to side-chambers increases from WD1 to WD21 in cocaine control mice (interaction Drug x Diet x WD:  $F_{(1, 77)} = 7.785$ ,  $p < 0.05$ ). (I) Crossing frequency during the test at WD21 time point (interaction Drug x Diet:  $F_{(1, 77)} = 4.297$ ,  $p < 0.05$ ). For convenience, behavioral data from mice in the first behavioral experiment and subsequent experiments (Fig.2) are pooled together (saline control  $N = 16$  mice, saline PLX  $N = 17$  mice, cocaine control  $N = 23$  mice, cocaine PLX  $N = 25$  mice). Data are presented as mean  $\pm$  SEM. Scale bars = 50  $\mu$ m. The symbols indicate, &  $p < 0.05$  compared to control diet, #  $p < 0.05$  compared to saline, ‡  $p < 0.05$  cocaine control WD1 vs cocaine control WD21, \*  $p < 0.05$

compared to saline control, saline PLX and cocaine PLX, \$ p<0.05 compared to cocaine PLX, by using Tukey's test for multiple comparisons).

Author Manuscript

Author Manuscript

Author Manuscript

Author Manuscript

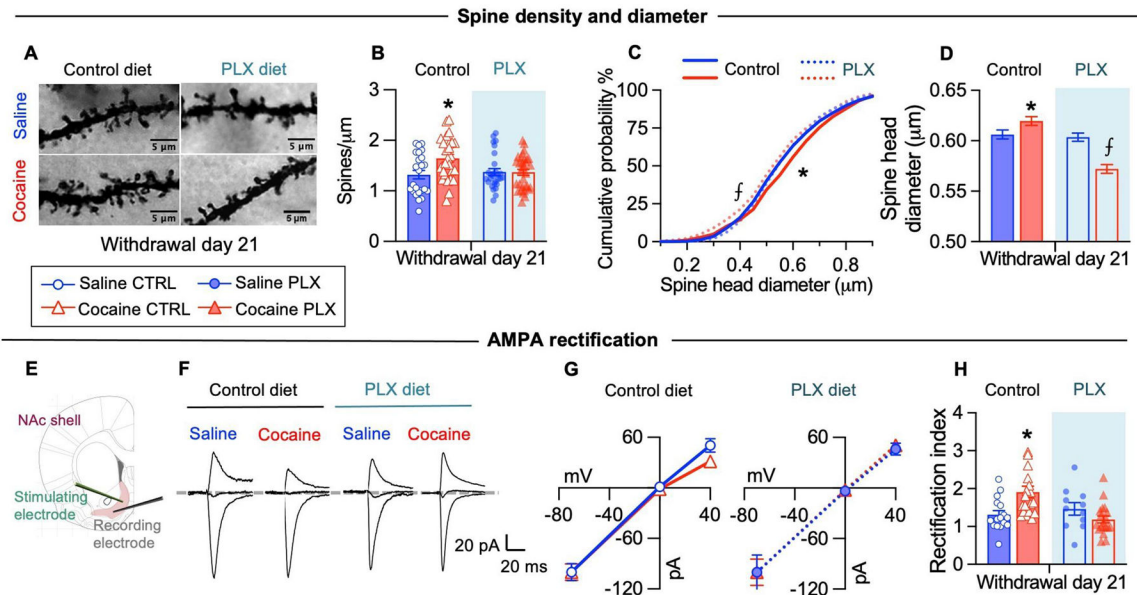


**Figure 2. Microglia depletion during cocaine withdrawal prevents dendritic spine changes and CP-AMPA accumulation in the nucleus accumbens shell**

(A) Representative images of Golgi-stained dendritic segments containing spines of NAc shell MSNs at WD21 under the indicated conditions. (B) Dendritic spine density in distal dendritic segments was higher in cocaine control mice at WD21 (interaction Diet x Drug:  $F_{(1, 108)} = 5.357$ ,  $p < 0.05$ ;  $N = 24\text{--}32$  segments/6–8 mice per group). (C) The cumulative distribution of the spine head diameter shows a significant rightward shift for the cocaine control group, indicative of wider spine diameters across the distribution, while it shows a significant leftward shift in the cocaine PLX group, indicative of smaller spine diameters across the distribution (K–S test (1949 spines/6–8 mice per group): cocaine control vs saline control ( $D = 0.08258$ ,  $p < 0.05$ ), cocaine control vs saline PLX ( $D = 0.08281$ ,  $p < 0.05$ ), cocaine control vs cocaine PLX ( $D = 0.1290$ ,  $p < 0.05$ ), cocaine PLX vs saline control ( $D = 0.06191$ ,  $p < 0.05$ ), cocaine PLX vs saline PLX ( $D = 0.08297$ ,  $p < 0.05$ )). (D) The average spine head diameter in MSNs distal dendritic segments at WD21 differs between cocaine control and cocaine PLX (Group:  $F_{(3, 7792)} = 22.74$ ,  $p < 0.05$ ). (E) Schematic depicting whole-cell patch clamp recordings from NAc shell MSNs. (F) Example traces of AMPA EPSCs evoked at  $-70$  mV,  $0$  mV, and  $+40$  mV for rectification index. (G) Average current-voltage relationship curves of evoked AMPAR-EPSCs. (H) The rectification index is higher in NAc MSNs of cocaine control mice (interaction Drug x Diet:  $F_{(1, 63)} = 9.184$ ,  $p < 0.05$ ;  $N = 11\text{--}16$  cells/6–7 mice group). Data are presented as mean  $\pm$  SEM. Scale bars =  $5 \mu\text{m}$ . The symbols indicate, \*  $p < 0.05$  compared to saline control, saline PLX and cocaine PLX,  $f$   $p < 0.05$  compared to saline control, saline PLX and cocaine control.

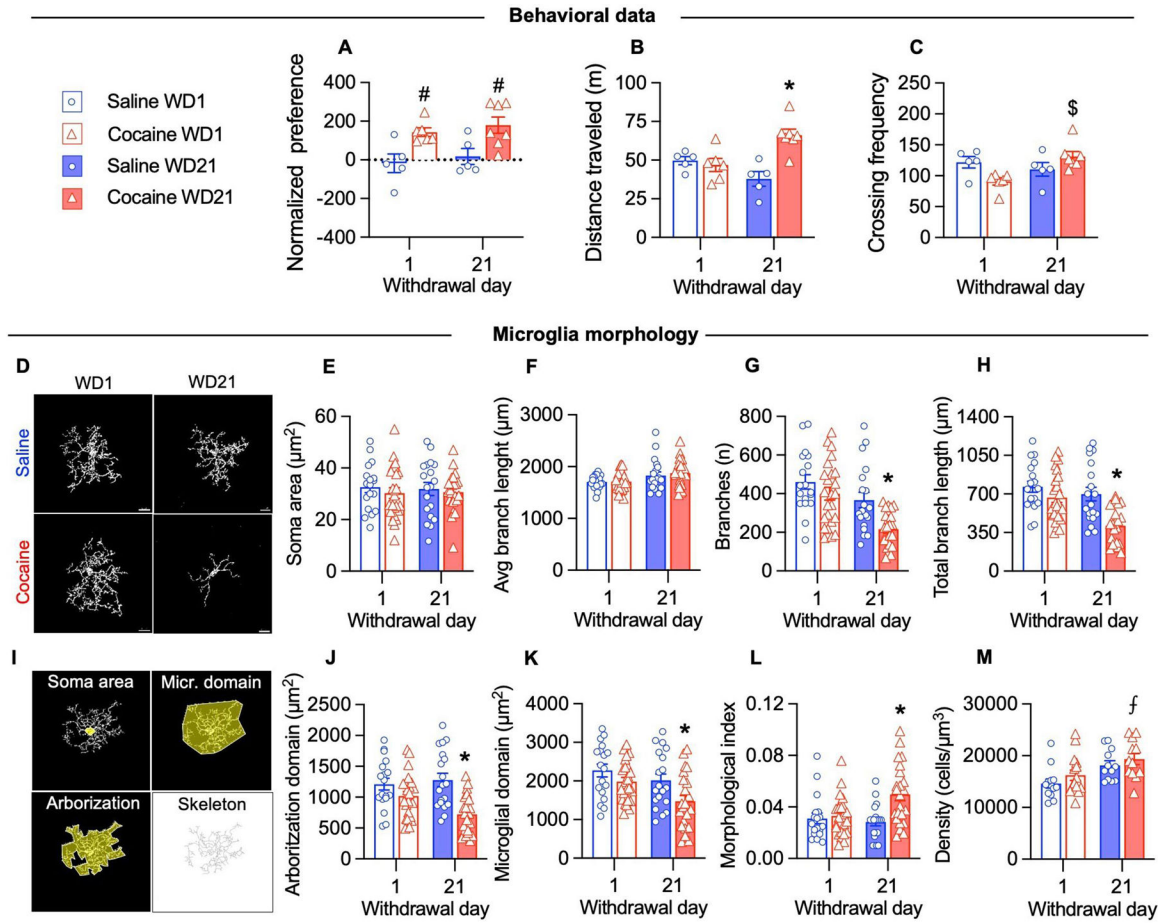


**Figure 3. Microglia display reduced branching after prolonged cocaine withdrawal.**

(A) Place preference score was higher in cocaine-treated mice compared to saline-treated mice both when tested at WD1 and at WD21 (Drug:  $F_{(1, 19)} = 16.41$ ,  $p < 0.05$ ). (B) The distance traveled in the apparatus was higher in cocaine-treated mice tested at WD21 compared to cocaine-treated mice tested at WD1 and saline groups (Drug x WD:  $F_{(1, 19)} = 14.69$ ,  $p < 0.05$ ). (C) The number of crossings between chambers in the apparatus was higher in cocaine-treated mice tested at WD21 compared to cocaine-treated mice tested at WD1 (Drug x WD:  $F_{(1, 19)} = 9.104$ ,  $p < 0.05$ ). (D) Representative images of microglia in the NAC shell at WD21 under the indicated conditions. (E-F) The microglial soma area ( $\mu\text{m}^2$ ) and the average branch length ( $\mu\text{m}$ ) did not change after cocaine CPP (two-way ANOVA Drug x WD,  $p > 0.05$ ). (G-H) The number of microglia branches (WD:  $F_{(1, 80)} = 17.91$ ,  $p > 0.05$ ; drug:  $F_{(1, 80)} = 10.46$ ,  $p > 0.05$ ) and total branch length (WD:  $F_{(1, 80)} = 11.15$ ,  $p > 0.05$ ; drug:  $F_{(1, 80)} = 15.78$ ,  $p > 0.05$ ) were reduced on WD21 after cocaine CPP. (I) Illustration of the morphological parameters used for quantification. Skeleton was used to determine branch length and number (J-K) The arborization domain (Drug:  $F_{(1, 80)} = 20.11$ ,  $p > 0.05$ ; Drug x WD:  $F_{(1, 80)} = 4.875$ ,  $p > 0.05$ ) and microglia domain (WD:  $F_{(1, 80)} = 6.905$ ,  $p > 0.05$ ; Drug:  $F_{(1, 80)} = 8.105$ ,  $p > 0.05$ ) were reduced on WD21 after cocaine CPP. (L) The morphological index, calculated as the ratio between the area of the soma and the arborization domain, is increased on WD21 after cocaine CPP (Drug:  $F_{(1, 80)} = 20.11$ ,  $p > 0.05$ ; Drug x WD:  $F_{(1, 80)}$

= 4.875 ,  $p > 0.05$ ). (**J**) Microglia density was increased in cocaine treated mice on WD21 compared to saline mice on WD1 (Drug:  $F_{(1, 48)} = 11.91$ ,  $p > 0.05$ ; 12–15 fields/3–4 mice/group). For the morphological analysis 18–24 cells/3–4 mice/group were analyzed. Data are presented as mean  $\pm$  SEM. Scale bars = 10  $\mu\text{m}$ . The symbols indicate, #  $p < 0.05$  compared to saline groups, \*  $p < 0.05$  compared to saline WD1, cocaine WD1 and saline WD21, \$  $p < 0.05$  compared to cocaine WD1, ‡  $p < 0.05$  compared to saline WD1.

Author Manuscript

Author Manuscript

Author Manuscript

Author Manuscript